COBEM-2017-1512
FATIGUE CHARACTERIZATION OF THE C36000 COPPER ALLOY USING THE THERMOGRAPHIC METHOD

Lucas Lira Lopez Rego
Jaime Tupiassú Pinho de Castro
José Luiz de França Freire
Vitor Eboli Lopes Paiva

Mechanical Engineering Department, Pontifical Catholic University of Rio de Janeiro (PUC-Rio), Rua Marquês de São Vicente 225, Rio de Janeiro, RJ 22453-900, Brazil
lucaslira20@hotmail.com; jtcastro@puc-rio.br; jlfreire@puc-rio.br; vitoreboli@hotmail.com

Abstract. *Even though the use of thermography as a non-destructive testing method is relatively well known, its use as a reliable tool for measuring the fatigue properties of metals is not. However, analyzing the temperature rise on the external surface of a structural component during cyclic loading can provide a reliable measure of its fatigue limit, avoiding the need for destructive tests and requiring much less time than standard test methods. It's also possible to determine the SN curve and the influence of the mean stress on its behavior through the same methodology, correlating an energy parameter with the assumption of its dependency on the stress amplitude. The results presented here show good agreement between the predicted and measured fatigue limits and mean stress influenced SN curves.*

Keywords: IR Thermography, Risitano Method, Fatigue Limits, Fatigue curves.

1. INTRODUCTION

Reliable fatigue properties are almost indispensable when designing structural components for long operational lives, as usual in many if not most practical applications. However, measurements of such an important data are so laborious that rarely, if ever, fatigue limits and fatigue curves are properly measured by design engineers in practice. Traditional methodologies, like Dixon's up-and down sequential method and Prot's incremental steps method need to test many fatigue specimens that do not break after lives longer than the lives estimated for the fatigue limits (Castro and Meggiolaro, 2016). Therefore, even for steels, for which fatigue limits can be associated to lives in the order of 10^6-10^7 cycles, but especially for many non-ferrous alloys, for which they can be as long as $5 \cdot 10^8$ cycles, the measurement of fatigue properties by traditional tests are expensive and always take a long time. Analogously, the conventional approach to determine fatigue curves requires a series of tests under different stresses levels with many replications, due to the relatively high dispersion of fatigue crack initiation data. Using this conventional approach, a life span of fatigue for each stress level can be estimated to produce a group of SN curves with varying levels of probability. Due to these difficulties, it is probably a truism to affirm that most long life designs use estimated instead of properly measured fatigue data, even for steel components, which tend to reach fatigue limits at relatively short lives.

However, such laborious traditional tests are not the only way to reliably measure fatigue properties. Indeed, since fatigue failures are associated to a transition from a conservative and non-damaging state to a dissipative and damaging one under cyclic loads, it can be expected that this transition can be associated to an increase in temperature at the location where a fatigue crack is in the process of being initiated. That is the basis for the thermographic method, which uses a suitable thermal camera to measure small temperature increments on the surface of fatigue specimens loaded under a series of incremental constant amplitude load steps, to identify the transition from the non-damaging state, below the fatigue limit, to the damage accumulation state above it. A methodology to perform such measurements has been recently proposed and tested (Fargione *et al.,* 2002; Freire *et al.,* 2015; La Rosa and Risitano, 1999; Vieira, 2016; Bandeira et al., 2017), and it is used here to characterize the fatigue properties of a C36000 Cu alloy (commercially known as Free-Cutting brass), commonly used in deep drawn structural components.

The thermographic method reduces the testing costs by decreasing the quantity of required specimens, but it is especially useful because it significantly decreases the testing time. Although realistic measurements of the fatigue limit are often obtained, this approach may still generate questionable results, in particular if used without the necessary precautions. Fatigue limits reported in literature using thermography analyses show variations up to ~20% when

compared with Dixon's up-and-down method, depending on the material, equipment and testing conditions, (Cura *et al.*, 2005), but the variations may be much smaller (Bandeira et al., 2017).

2. IR THERMOGRAPHY METHOD

The IR thermography is a technique that allows the thermal mapping of the surface of a body or a region through the use of a sensible thermal camera, with the intention of distinguishing areas with different temperatures, in particular the small ones. It is, therefore, a technique that allows artificial visualization of light within the infrared spectrum. It is within the group of techniques known as nondestructive (NDT), real-time and non-contact.

The methodology proposed by La Rosa and Risitano (1999), which is also known as Risitano Rapid Method (RRM), states that it is possible to evaluate the dynamic behavior of the component and to determine the fatigue limit of the material by analyzing the external surface temperature of suitable specimens during cyclic loading. This method does not need any particular testing machine and obtains reliable results using a limited number of specimens in a very short time, because it can detect incipient fatigue damage without needing to break the fatigue specimens.

When the specimen is loaded below the fatigue limit, its temperature varies very slightly due to the thermoelastic effect, but for stress amplitudes above the fatigue limit the temperature variations are significant. The temperature increments (ΔT) behavior has three phases. They increase during the first part of the test (phase 1), then remain stable for a while (phase 2), and finally rapidly increase prior to failure at a life of N_f cycles (phase 3), as shown in Fig. 1.
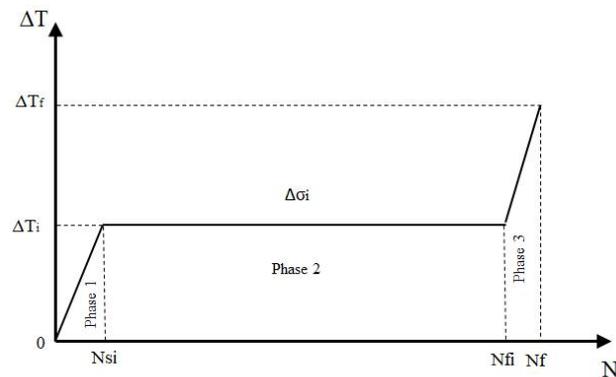

Figure 1: Phases of the thermal behavior of ΔT vs. N curve for a hot spot in
the specimen surface during typical fatigue tests, adapted from (Fargione *et al.,* 2002).

Through the analysis of the temperature response curve under incremental cyclic step loading, see Fig. 2A and 2B, the fatigue limit can be evaluated considering the heating rate ($\Delta T/\Delta N$) or the stabilized temperature increment ΔT_i (La Rosa and Risitano, 1999). Each stress amplitude level corresponds to one stabilization temperature. Two linear regression lines are used to approximate the thermal data and to determine graphically the fatigue limit, as depicted in Fig. 2B. The first line contains the data where the applied stress is below the fatigue limit, and the second line fits the data located above the limit. The fatigue limit is determined by the intersection of these two lines, as shown in Fig. 2B. For stress amplitudes below the fatigue limit, the small temperature increments ΔT are caused by thermoelastic effects, thus they increase only until a steady-state ΔT_i is reached without failure (La Rosa and Risitano, 1999).
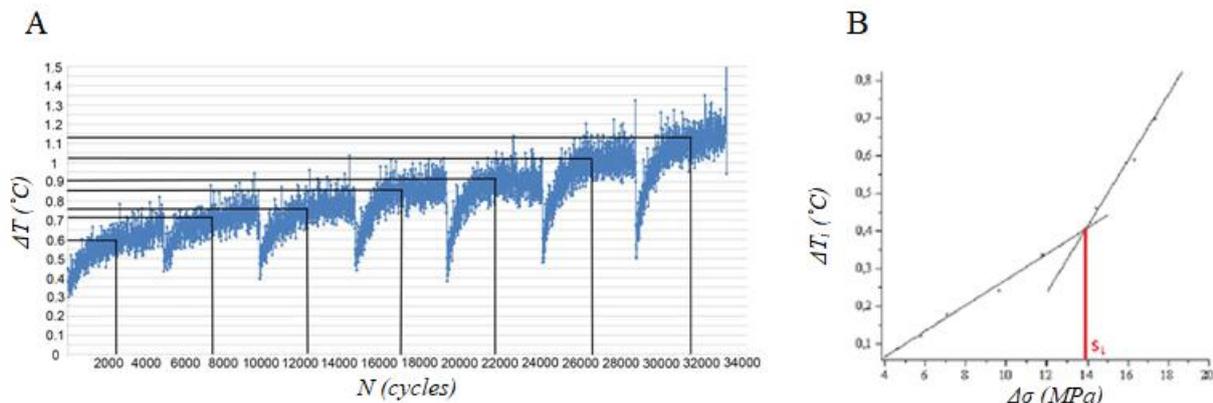

Figure 2: A) ΔT vs. N curve for various stress amplitudes $\Delta\sigma_i$, with the determination of each ΔT_i;
B) ΔT_i vs. $\Delta\sigma_i$ curve for various incremental load steps.

Using the same line of analysis, Fargione *et al.* (2002) proposed a method to determine the fatigue-life curve of the material using IR thermography. This method is much faster than the traditional one and needs theoretically only one specimen. In practice, three is the recommended minimum number of specimens. This method correlates the plastic deformation energy density (E_C) with material failure, as seen in Eq. (1):

$$E_C = \int_0^{N_f} E_P dN \tag{1}$$

where E_C is the amount of micro-plastic strain energy to failure per unit of volume (a property of the material), N_f is the number of cycles to failure, and E_P is the energy due to yielding per unit volume per cycle.

The work done over the system by the loading (E_W), as presented in Eq. (2), results from the stored internal energy (E_i) and the energy converted into heat (Q).

$$E_W = E_i + Q \tag{2}$$

Assuming E_i to be small compared to Q, and using Risitano's results, which have shown E_W to be proportional to E_p, Fargione *et al.* (2002*)* proposed:

$$E_C = \int_0^{T_f} dQ \tag{3}$$

For small temperature variations (under 100K, implicating small loading frequencies), the heat transferred from the specimen to the environment can be considered proportional to the temperature difference ΔT. Because of that, Q can be evaluated through a parameter ϕ, which is the integral of the ΔT vs. N curve in Fig. 1, Eq. (4):

$$\phi = \int_0^{N_f} \Delta T dN \tag{4}$$

In practice, ϕ is assumed constant for given test conditions, such as the specimen geometry and material, loading frequency and environment. This critical value corresponds to fatigue failure and it is associated to the total area under the curve in Fig. 1 (for one constant stress amplitude level), or the total dashed area in Fig.3 (for several stress amplitude levels). The ϕ value can be used together with measurements of ΔT_i, ΔT_{0i}, ΔN_i at the various stress amplitude levels for a single specimen, as depicted in Fig. 3 and modeled by Eq. (5) and Eq. (6), to yield the whole fatigue SN curve. Each data point of the SN curve is formed by the pair (N_{fi}, $\Delta\sigma_i$) where N_{fi} is calculated from Eq. (5). This equation is derived with the help of Fig.3 and the assumption that phase 3 depicted in Fig. 1 is small and can be neglected. The value of N_{si} is determined from Eq. 6 with the help of Fig. 3.

$$\phi = \Delta T_i \left(N_{fi} - \frac{\Delta N_{si}}{2} \right) \tag{5}$$

$$N_{si} = \frac{\Delta N_i \Delta T_i}{\Delta T_i - \Delta T_{0i}} \tag{6}$$

The partial damage value D_i results from the partial integrated value ϕ_i resulting from the application of each stress amplitude $\Delta\sigma_i$. The value ϕ_i is calculated considering the number of cycles applied at each stress level, N_{pi}. The denominator of Eq. (7) gives the area under the curve ΔT vs. N considering the interval N_{pi}. The partial damage value of Eq. (7) assumes Miner's linear damage accumulation rule is valid.

$$D_i = \frac{\phi_i}{\phi} = \frac{\left(\dfrac{\Delta T_i + \Delta T_{0i}}{2} \right) \Delta N_i + \Delta T_i \left(N_{fi} - \Delta N_{si} \right)}{\displaystyle\sum_1^f \phi_f} \tag{7}$$
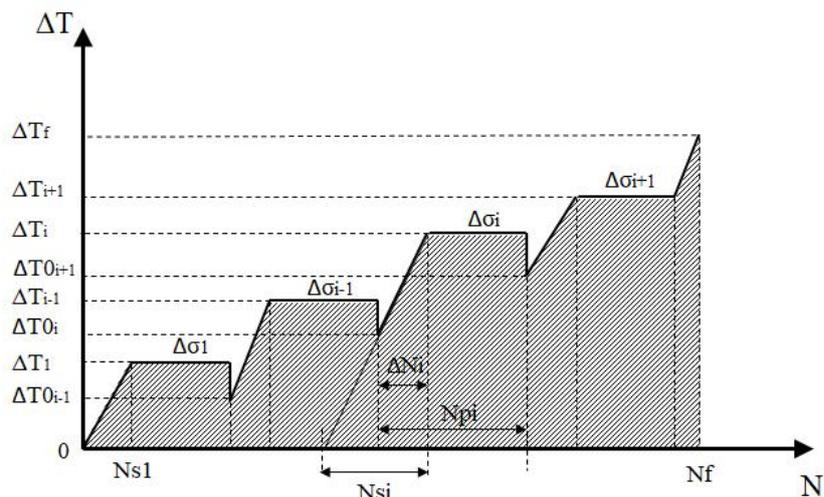
Figure 3: Stepped loading procedure for the determination of the fatigue limit and the integral ϕ.

3. MATERIAL AND EXPERIMENTAL PROCEDURE

Seven cylindrical specimens made from a C36000 Cu alloy, commercially known as Free-Cutting brass, were tested to evaluate their fatigue behavior using the proposed method. One specimen is presented in Fig. 4. The diameter of the uniform gage test section was 10.0 mm, a value verified by the mean of five measurements taken with a micrometer. The chemical composition of this brass was furnished by its supplier, and it is presented in Tab. 1, while its basic mechanical properties are shown in Tab. 2. These properties were measured in a 100 kN machine with a crosshead speed of 0.9 mm/min according to ASTM E 8M−13a standard (ASTM, 2013) procedures (Nóbrega, 2010).

Figure 4: Brass specimen tested.

Table 1: Chemical analysis according to ASTM E30 and ASTM E663, see (Nóbrega, 2010).

Element	Cu	Zn	Pb	Fe	Sn	P	Al	Mn
(%)	61,63	35,10	2,92	0,14	0,10	0,010	<0,01	<0,01

Table 2: Measured mechanical properties.

Properties	Measured	Obtained from the literature (Nationalbronze, 2017)
Tensile Strength [MPa]	436	450
Rockwell B Hardness	72	70

The preparation of specimens for thermographic analysis is described by Charles *et al.* (1975). All specimens were painted with a thin layer of opaque black paint to increase their emissivity, making it close to the value of a black body. The specimens were fatigue tested in a 100 kN INSTRON 8501 servo−hydraulic machine, Fig. 5.

During each fatigue test, the surface temperature was recorded in real time by a microbolometer thermocamera FLIR A655sc, see Fig. 6A. It uses a focal plane array (FPA) of 640×480 pixels, and has spatial resolution of 17 μm, acquisition frequency of 50 Hz on full frame configuration, spectral range from 7.5 to 14 μm, and sensitivity below 30 mK. Temperature data was acquired and analyzed using the ResearchIR software from FLIR. The thermal profile for the first specimen is shown in Fig. 6B. Environment temperature and heating associated to the loading machine can contribute to increase the surface temperature of specimen (De Finis *et al.*, 2015). In this work, the later factor could be neglected due to the large dimensions of the testing machine and of the grips, the relatively low frequency of the tests, and the low number of cycles for each load step ($\approx 5 \cdot 10^3$). A reference body placed aside the specimen for temperature compensation purposes confirmed the testing system had a negligible effect on the fatigue specimens.
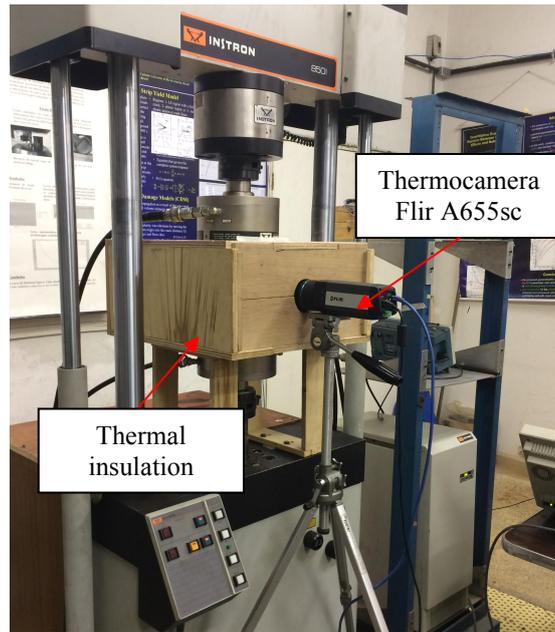
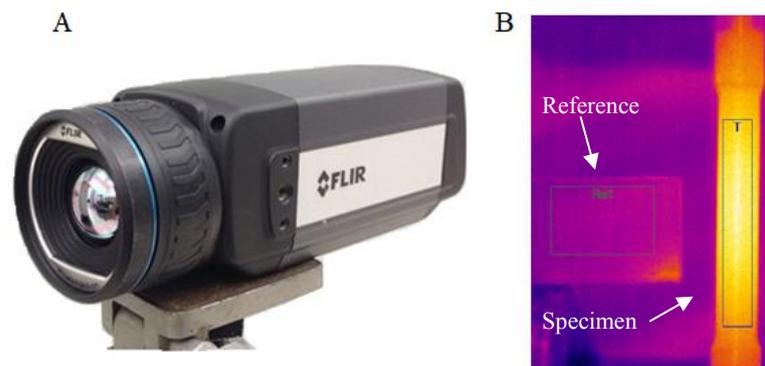Figure 5: INSTRON servo−hydraulic machine during the test.

Figure 6: A) Camera FLIR A655sc; B) Reference and specimen areas and thermal profile
used to measure the specimen surface temperature in the fatigue tests.

Based on the experimental methodology proposed by De Finis *et al.* (2015), the specimens were tested under a step loading procedure, sequentially applying to each specimen at a constant amplitude under force-control, with stress ratios $R = \sigma_{min}/\sigma_{max}$ equal to $R = −1, −0.5, 0.1$ and 0.5. At each load step, the load amplitude was maintained fixed during blocks of $5 \cdot 10^3$ cycles, a value that was high enough to achieve a stable thermal behavior, as determined by preliminary tests. Afterwards, the load was increased until the specimen failed.

4. RESULTS AND DISCUSSION

The temperature variation with number of cycles and applied stress amplitude are presented respectively in Fig. 7 and Fig. 8. These plots show that the temperature undergoes a significant increase when it is submitted to elevated stress levels, above the fatigue limit. Figure 7 shows that temperature stabilizes around 1000 cycles for each stress level, completing the transition from phase 1 to phase 2, as shown in Fig. 1. Fig. 7 shows that after reaching temperature stabilization, the cyclic loading is kept for approximately 5000 cycles until the test stress level is changed. This way the specimen is consecutively loaded until it finally reaches phase 3 (failure).

Fig. 8 shows the stabilized temperatures, ΔT_i, obtained from Fig.7, plotted against their corresponding amplitude stress levels, $\Delta \sigma_i$. According to Ristanos' method, the fatigue limit S_L can be determined graphically by the intersection of two regression lines based on the data below and above the fatigue limit, as illustrated in Fig. 8. When the specimen is subjected to a stress amplitude above the fatigue limit, its temperature increases significantly and damage begins to accumulate in the specimen until the formation of a crack leads it to an eventual failure. The fatigue limit $S_L = 139$ MPa determined for specimen 2 under $R = −1$ determined in Fig. 8 may be compared with typical values listed in Castro and Meggiolaro (2016), for copper alloys from 25% to 50% of their tensile strength, 109 to 218MPa for the tested alloy. The measured fatigue limit is inside this range.
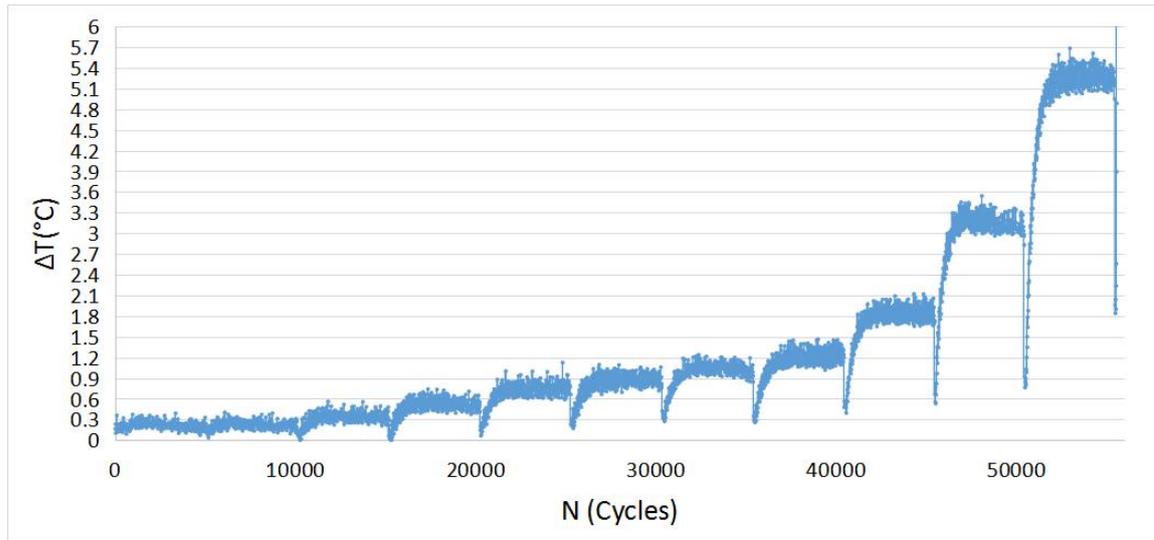
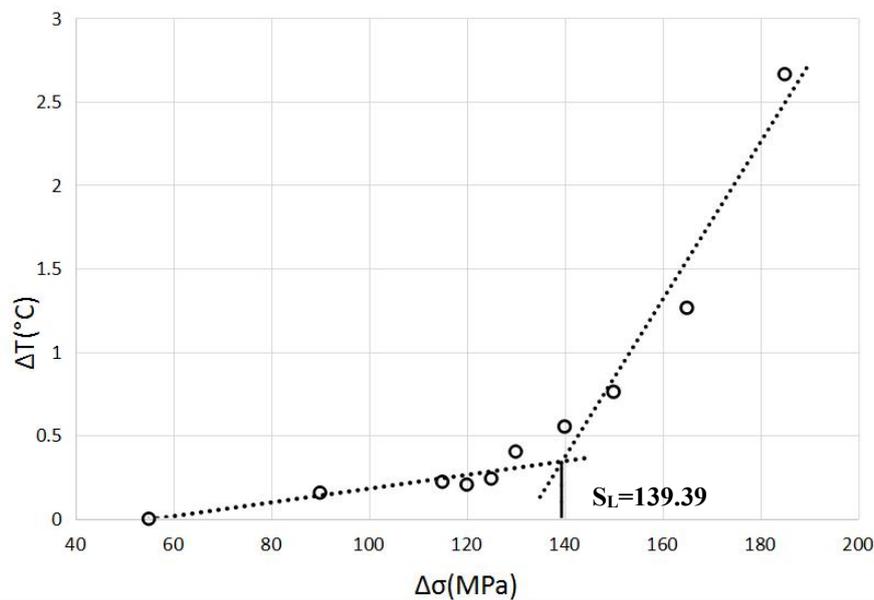Figure 7: Average temperature variation measured during a test.

Figure 8: Intersecting lines showing the fatigue limit for test 2 (R= −1).

Seven specimens were tested at four different stress ratios ($R = \sigma_{min}/\sigma_{max}$). Test results are summarized in Tab. 3 and Tab. 4. As shown by Guamán *et al.* (2017), the use of low test frequencies (between 5 and 25Hz) do not affect the measured results. In the present case, three different frequencies were used during the tests (5, 10, and 15Hz). The comparison between the test results using different frequencies shows similar fatigue limits, as it can be seen in Tab. 3.

Table 3: Measured results for each specimen.

Specimen	Fatigue limit S_L (MPa)	R	Frequency (Hz)	N_P (cycles)	ϕ (°C·cycles)	D (from Eq. (7))
1*	135.01	−1	15	-	-	-
2	139.39	−1	5	71981	689389.90	0.96
3	122.10	0.1	10	55637	67347.96	0.99
4	119.17	0.1	15	56193	93736.32	0.99
5	131.72	−0.5	15	71550	562041.37	0.97
6	79.95	0.5	15	60975	71292.08	0.99
7	84.21	0.5	15	63337	85012.16	0.94

*Specimen 1 was not tested until failure.

Table 4: Average fatigue limit for each tested R.

R	Average Fatigue Limit	Curve Adjusted Fatigue Limit
−1	137.20	138.00
−0.5	131.72	136.50
0.1	120.64	121.89
0.5	82.08	87.72

Based on the average fatigue limit presented in Tab. 4 for each applied R, data points formed by pairs of alternate stress amplitude values (σ_a) and mean stresss (σ_m) were calculated and plotted in Fig. 9. The resulting data was adjusted by a parabolic fitting equation presented in Eq. (8), the adjusting exponent α being equal to 1.65. It can be seen that the data of the thermographic tests were well adjusted for the calculated exponent, which is between the exponents given by the so called Goodman and Gerber curves, respectively equal to 1 and 2 (Castro and Meggiolaro, 2016).

$$\frac{\sigma_a}{S_L} + \left(\frac{\sigma_m}{S_u}\right)^\alpha = 1$$
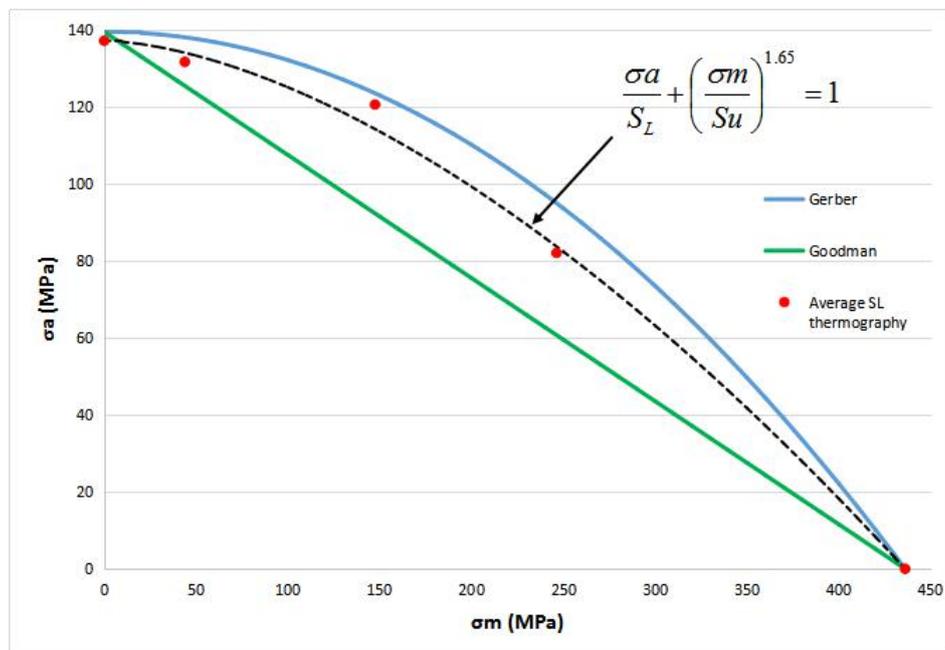
(8)

Figure 9: Graphic alternate stress vs. mean stress for Gerber, Goodman and thermographic.

Having determined the values of ϕ as presented in Eq. (5) and Eq. (7), the *SN* fatigue curve can be determined using the process outlined in section 2. The *SN* fatigue curves for each stress ratio R calculated in this way are presented in Fig. 10. The calculated curves encompass data fitted to the interval 10^4 to 10^6 cycles. It can be seen that the fatigue curves for $R = −1$ and $R = −0.5$ are very similar.

5. CONCLUSIONS

This paper confirms that Risitano's method (La Rosa and Risitano, 1999) is a practical and efficient tool that can provide a reliable and fast way to determine the fatigue behavior of materials using few specimens. More specifically, the paper furnishes fatigue data for the C3600 free-cutting brass alloy, which is scarce in the literature. Moreover, the influence of the stress ratio R was evaluated for this material and an equation showing the influence of the mean applied stress on the fatigue limit was given, which can be useful for design purpose.
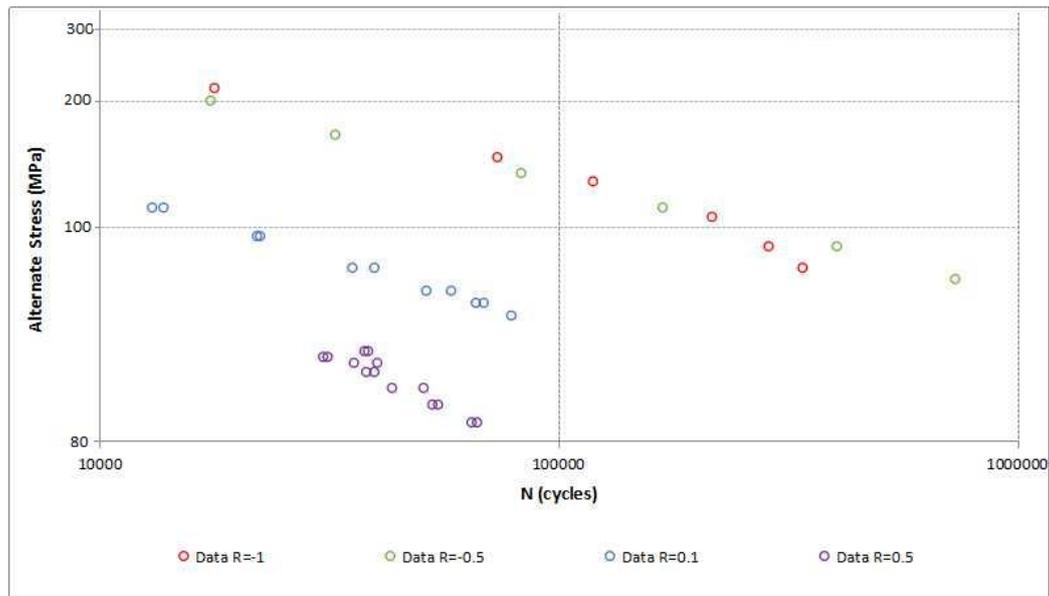
Figure 10: Fatigue curve for each stress ratio.

6. REFERENCES

ASTM E 8M−13a, 2013. "Standard Test Methods for Tension Testing of Metallic Materials" *American Society for Testing and Materials*, USA.

Bandeira C. F. C., Kenedi P. P.; Castro J. T. P., Meggiolaro M. A., 2017. "On the use of the thermographic technique to determine the fatigue limit of a cold drawn carbon steel". *Seventh International Conference on Very High Cycle Fatigue*, p.329-334, U. Siegen. ISBN 978-3-00-056960-9.

Castro J. T. P., Meggiolaro M. A., 2016. "Fatigue Design Techniques, volume 1: High-Cycle Fatigue.." CreateSpace.

Charles, J.A., Appl, F.J., Francis, J.E., 1975. "Using the scanning infrared camera in experimental fatigue studies", *Experimental Mechanics*, Vol. 15, p. 133–138.

Cura, F., Curti, G., Sesana, R., 2005. "A new iteration method for the thermographic determination of fatigue limit in steels", *International Journal of Fatigue*, Vol. 27, p. 453–459.

De Finis, R., Palumbo, D., Ancona, F. and Galietti U., 2015., "Fatigue limit evaluation of various martensitic stainless steels with new robust thermographic data analysis", *International Journal of Fatigue*, Vol.74, p. 88−96.

Fargione G, Gerarci A, La Rosa G, Risitano, 2002. A. Rapid determination of the fatigue curve by the thermographic method. *International Journal of Fatigue*, Vol. 24, p. 11-19.

Freire J. L. F., Waugh R. C., Fruehmann, R., Dulieu-Barton J. M., 2015. Using thermoelastic stress analysis to detect damaged and hot spot areas in structural components. J. Mech. Eng. Autom, Vol. 5, p. 623-634.

Guamán A., Castro J. T. P., Vieira R. B., Paiva V. E. L., Freire J. L. F., 2017. "Fatigue Limit Assessment of a Low Carbon Steel using Dixon's Up-And-Down and Infrared Thermography Methods" International Conference on Advances in Experimental Mechanics 29th - 31st August 2017, University of Sheffield, UK.

La Rosa G, Risitano A., 1999. Thermographic methodology for the rapid determination of the fatigue limit of materials and mechanical components. *Int J Fatigue Mater Struct Components* 1999; Vol. 22, p. 65-73 [December].

Nationalbronze <www.nationalbronze.com/pdfs/C36000.pdf> 2017. (last acessed 29.09).

Nóbrega M. J. R., 2010. "Influência da metodologia de medição das propriedades mecãnicas dinâmicas na previsibilidade do comportamento de estruturas sujeitas a impactos elastoplásticos" *PhD Thesis*, Pontifícia Universidade Católica do Rio de Janeiro, Departamento de Engenharia Mecânica.

Vieira R. B., 2016. "Thermography applied to the study of fatigue in polycarbonate", *MSc. Thesis,* Pontifícia Universidade Católica do Rio de Janeiro, Departamento de Engenharia Mecânica.

.

7. RESPONSIBILITY NOTICE

The authors are the only responsible for the printed material included in this paper.